Fluorescence spectroscopy analysis of fly ash removal from aqueous systems: adsorption of alginate to silica and alumina

ARTICLE

Fluorescence Spectroscopy Analysis of Fly Ash Removal from Aqueous System: Adsorption of Alginate to Silica and Alumina

[l]Received 00th January 20xx,
Accepted 00th January 20xx

DOI: 10.1039/x0xx00000x

Fateh Eltaboni,*[a] Sehaj Singh[c], Linda Swanson[b], Thomas Swift [c] and Abdulraheem SA Almalki [d]

Fly ash is a toxic industrial waste, mainly consisting of silica and alumina aparticles, that has been found discharged into the environment. It is proposed that alginate, a naturally occuring biopolymer, can bind to these minerals and thus play a role in water purification. The binding forces involved in this process consist of weak interactions, such as Van der Waals's forces and electrostatic interactions. Although attachment of alginate to mineral surfaces is mainly governed by its carboxylate groups, hydroxyl moieties could play a role in the interaction between polymer and minerals. This work aims to use the SiO_2 and Al_2O_3 particles as a model for fly ash and show the use of alginate biopolymers (fluorescently labelled with an aminonaphthaline sulfonate fluorophore (AmNS)) to coagulate them. The addition of simple electrolytes like NaCl and $CaCl_2$ encourages the coiling of the polymer chain at high pH values which has an effect on its capability to bind to the inorganic particles. A combination of fluorescence and ICP-MS demonstrated that alginate had a considerable adsorption affinity for Al_2O_3, whereas it attracts weakly to the SiO_2. The adsorption process is pH dependent: strong adsorption was observed at low pH. The dependence of adsorption on the minerals (Al_2O_3 and SiO_2) concentration was also examined at different pH conditions: the adsorption amount was observed to increase by increasing the solid concentration. Adsorption isotherms obtained at low and high mineral concentrations were found to be Henry in type.

Introduction

Fly ash is a particulate pollutant emitted from thermal power plants produced as a result of coal burning or biomass combustion.[1] Disposal of fly ash is a currently a burning issue as it has been considered as a significant organizational restriction and environmental health threat.[2] Migration of contaminants from ash disposal sites to soil and groundwater, has recently been the interest of several researchers worldwide. Silica (SiO_2) and alumina (Al_2O_3) are the main constituents of fly ash, which have a great affinity to heavy metals, resulting in the spread of environmental pollution. In recent years, numerous studies have been carried out to address the disposal, and potential reuse, of fly ash waste and mitigate its environmental impact.[3–10] These studies include ion-exchange, flocculation, membrane filtration, coagulation, enzymatic decomposition, advanced oxidation, and adsorption methods.[11,12] All these methods are now used in several applications, with varying success rates. Among them, adsorption is considered a more practicable alternative because of its ease of operation, simplicity, ability to respond quickly to varying conditions like pH of system, non-toxicity and high efficiency. For example, eco-friendly adsorbent consisting of natural polymers was introduced to investigate macromolecule-fly ash adsorption.[13] The use of polysaccharides appears to be an ideal alternate for the removal of fly ash waste in water decontamination. Among the industry-attractive polysaccharides, alginate is known to has high complexation affinity toward minerals like silica and alumina.[12–14]

Alginate was nominated as an adsorbent due to it is a natural, biocompatible, biodegradable, nontoxic and hydrophilic nature, making it an ideal candidate for the adsorption of the fly ash minerals. The understanding of alginic acid behaviour in aqueous solution begins with an understanding of the basic chemistry. Alginate, also known as alginic acid is a linear polymer isolated from brown seaweeds or soil bacteria. This polysaccharide is composed of (1→ 4) linked β-D-mannuronic acid (M) and its C-5 epimer, α-L-guluronic acid (G).[15–20] The natural random biopolymer formation produces different quantities of G-block, M-block and MG-block. The M/G ratio

[a.] *Department of Chemistry, University of Benghazi, Benghazi, Libya.*
[b.] *Department of Chemistry, The University of Sheffield, Sheffield S10 2TN, U.K.*
[c.] *School of Chemistry and Biosciences, University of Bradford, Bradford BD7 1DP, U.K.*
[d.] *Department of Chemistry, Faculty of Science, Taif University, Taif, Kingdom of Saudi Arabia*

† Footnotes relating to the title and/or authors should appear here.

Electronic Supplementary Information (ESI) available: Biopolymer characterisation, fluorescent properties of AmNS, interactions of AmNS with silica and alumina particles, additional fluorescence raw data for Alginate* and interactions of these systems with salts. See DOI: 10.1039/x0xx00000x

can affect mechanical properties and adsorption capacities of alginate gels[21] however in dilute solution they have similar lipophilicitys with pKa values of 3.38 and 3.65 for the M and G blocks respectively.[22] This means that the alginate chains can form hydrophilic-hydrophobic aggregates in aqueous solution by changing the pH of the medium.

Alginate has a unique physicochemical behaviour, which is affected by its composition and the environment surrounding it. Many studies have reported that the conformational behaviour of alginate is influenced by factors such as concentration, pH of the medium, ionic strength and the presence of some cations such as Ca^{2+}, Mg^{2+}, Na and K^{+}.[16,17,23–25] Luminescence has previously been used to track the conformational change of alginate with pH as it changes it's micro-environment from hydrophilic to hydrophobic as the pH is decreased from 6 to 4.[22] Despite this empirical research the molecular interactions of an aggregated alginate solution are not fully understood. It has been known that alginate can form gels at pH less than the pKa values of its respective monomers.[18,19,23] Alginic acid monomers contain carboxyl and hydroxyl groups that may interact with mineral surfaces. The carboxyl group can potentially interact with a surface via electrostatic forces, while the hydroxyl group may interact via hydrogen bonding.[26] The stability of biomacromolecules, such as alginic acid, when in presence of solid surfaces is influenced by the conformation adopted by these macromolecules.[27] However, the adsorption behaviour of alginates at molecular level is not fully understood.

With the aim of providing a molecular level understanding of fly ash mineral adsorption onto natural coagulant polymer, we study here the effect of aqueous chemical composition on the molecular conformation of alginate and its sorption to alumina and silica. It is hypothesised that the alumina and silica minerals mimic active sites existing on the surface of fly ash particles, which control the accumulation of fly ash waste in natural water systems. An approach was developed involving the synthesis of fluorescently labelled alginate from brown algae, and the use of fluorescence time resolved anisotropy measurements (TRAMS) to monitor the conformational behaviour of this biopolymer. This was achieved using the fluorescent-labelled 4-amino naphthalene-1-sulfonic acid (AmNS), which was covalently bound to the alginate backbone. AmNS has previously shown to be a reliable reporter of polymer conformation in the solution and has been used to study the adsorption of poly(acrylic acid) onto the surface of calcite[28] and lipopolysaccharide onto silica and alumina surfaces.[29] Adsorption of alginate was studied in dilute ionic solutions as a function of pH and in the presence of alumina and silica. This approach provides a mechanistic understanding of binding at the interface of the natural coagulant and minerals, a process vital to prevent fly ash growth in aqueous system.

The photophysical behaviour of the diluted aqueous solution of fluorescently labelled alginate and the corresponding model compounds were investigated using fluorescence spectroscopy. Fluorescence and potentiometric techniques are applied to study the effect of pH and ionic strength on the conformational behaviour of an alginate chain. The interaction of this biopolymer with silica and alumina is also studied. The adsorption isotherms of alginate on minerals were derived by determining aqueous aluminium and silica concentrations using inductively coupled plasma mass-spectroscopy (ICP-MS).

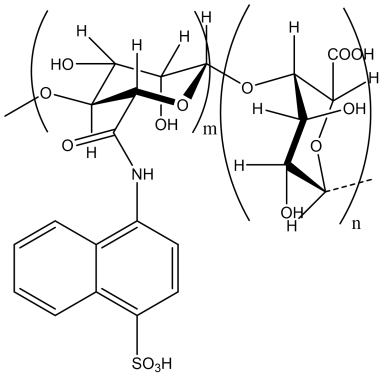

Scheme 1. Chemical structure of AmNS-labelled alginate, where n is two degrees of magnitude larger than m.

Materials and Methods

Materials. All materials were used as received unless otherwise stated. Dioxane (Aldrich, spectroscopic grade), Methanol (Aldrich, general and spectroscopic grades), Ethanol (Aldrich, general and spectroscopic grades), Diethyl ether (Aldrich general and spectroscopic grades), Water (double distilled), Tetrahydrofuran (Fisher, general grade), Dichloromethane (Fisher, HPLC grade), Dimethyl formamide (Aldrich, spectroscopic grade), Glycerol (Aldrich, spectroscopic grade), Potassium carbonate (Aldrich, 99%), Hydrochloric acid (Fluka, ≥ 37%), Sodium hydroxide (Sigma-Aldrich, ≥ 97%), Tri ethylamine (Aldrich, 99.5%), Triethyleneglycol monochlorohydrin (Aldrich, 96%), Aluminium oxide (50-200 micron) (Acros Organics), Sodium chloride (Sigma-Aldrich, ≥ 99.5%), Calcium chloride (Sigma, ≥ 96%), LUDOX® AS-30 colloidal silica 30 wt% suspension in H2O (Aldrich), N,N'-Dicyclohexyl carbodiimide (DCC) (Aldrich, 99%), Methacrylic acid (Aldrich, 99%), 4-(Dimethyl amino) pyridine (DMAP) (Aldrich, ≥99%), Sodium bicarbonate (Fluka, ≥ 99%), Anhydrous sodium sulphate (Sigma-Aldrich, ≥ 99%), N-Hydroxysuccinimide (Sigma-Aldrich, 98%), N-(3-Dimethylaminopropyl)-N'-ethylcarbodiimide hydrochloride (EDC) (Fluka, ≥99.0%) Used as received, without any further purification, N-hydroxysuccinimide (NHS) (Aldrich, 98%) Used as received, without any further purification. 4-amino naphthalene-1-sulfonic acid (AmNS) (Aldrich, 97%) 4-Amino naphthalene-1-sulfonic acid (AmNS) was purified by extraction with warm hexane, the residue was removed, the produced material having melting point 300 – 302 °C, which had been dried under vacuum over $CaCl_2$. Then it was stored in a dark

coloured bottle, in cold place. The product was isolated in ~ 74 %.

Alginate Purification. Alginate (5 g) was purified to remove sodium residue by dissolving in a stirring solution of NaOH (0.5 M, 25 ml). The solution was stirred for 2 hours before HCl (0.5 M) was added dropwise to bring the solution to pH 2.5 and then the solution was stirred for 24 hours. The resulting gel suspension was filtered in a quantitative filter paper and washed with ethanol, before being dried in a vacuum (40 °C, 24 hours).

Synthesis of AmNS-labelled alginate. The purified Alginate was labelled with 4-amino naphthalene-1-sulfonic acid (AmNS) with a slight modification according to the procedure described elsewhere.[30] Alginic acid (3 g, 18 mmol monosaccharide) was mixed with water (80 ml), 1,4-dioxane (30 ml), 4-Amino naphthalene-1-sulfonic acid (50 mg, 0.15 mmol) and N-(3-dimethylaminopropyl)-N'-ethylcarbodiimide hydrochloride (1.00 g, 7.8 mmol). The mixture was stirred for 3 hours and left overnight as the solution turned orange with some precipitate remaining on completion. The mixture was filtered and washed with acetone until the extraction was colourless, leaving a yellow powder that was dried and weighed. This was further purified by being ultrafiltered to remove low molecular weight residual substances. This was carried out using a 300 ml stirred cell (Millipore, UK) at 400 kPa nitrogen pressure with 70 mm cellulose 3000 MWCO filters. The procedure was carried out over ca. 1 hour to give a final volume of 20 - 50ml. After this process was repeated in triplicate the remaining liquid was removed via lyophilisation to produce a dry yellow powder that was characterised by NMR, GPC, FTIR, UV-vis absorbance and viscometry.

Alumina Particle Properties. Physical State: Crystalline white powder**.** Particle diameter: 1363.5±72.8 nm (DLS analysis)**.** Surface area: 1.11 m^2/g (Sigma-Aldrich)**.** pH: 8.5 (1 wt% in water) (pH-meter)**.** e.m.f: -94 mv (1 wt% in water) (Potentiometer)**.** Density: 3.97 g/cm^3 (Sigma-Aldrich)**.** Molecular Formula: Al_2O_3 (Sigma-Aldrich)**.** Molecular Weight: 101.96 g/mol (Sigma-Aldrich).

Silica Particle Properties. Physical State: colloidal, 30 wt. % suspension in water. Particle diameter: 34.7±1.4 nm (DLS analysis)**.** Surface area: 225 m^2/g (Sigma-Aldrich)**.** pH: 9.2 (1 wt% in water) (pH-meter)**.** e.m.f: -123 mv (1 wt% in water) (Potentiometer). Density: 1.21 g/cm^3 (Sigma-Aldrich). Molecular Formula: SiO_2 (Sigma-Aldrich). Molecular Weight: 60.08 g/mol (Sigma-Aldrich).

Instrumentation

Nuclear magnetic spectroscopy (NMR). To characterise the monomers, synthetic model polymers and biopolymers proton nuclear magnetic resonance (^{1}H NMR) spectra were recorded on a Bruker AC250 sample changer instrument operating at 400 MHz. The monomer and polymer samples were prepared in deuterated solvent (20 mg ml^{-1}). **Fourier transform infrared spectroscopy (FTIR).** FTIR spectra of polymer samples were recorded in absorbance with 10 scans using Perkin Elmer FTIR Spectrometer. All polymer samples were prepared for the measurements in the form of KBr disks. **Ultraviolet spectroscopy (UV).** A Hitachi U-2010 spectrometer was used to analyse the absorbance from 800 nm to 200nm with a scan speed of 400 nm min^{-1} with a slit width of 2 nm. Samples were prepared in dilute solutions in 1 cm quartz cuvettes. Fluorophores were measured at different concentrations in methanol spectroscopic grade, whereas polymer solutions at 10^{-1} wt% in deionised water were prepared and measured at room temperature. **Gel-permeation chromatography (GPC).** Average molecular weights of prepared macromolecules were determined by Gel Permeation Chromatography (GPC). Poly (ethylene oxide) (PEO) and poly (ethylene glycol) (PEG) were utilized as standards. The mobile phase was a 0.1M sodium nitrate and 0.01M sodium dihydrogen phosphate aqueous solution. The mobile phase was run through two Viscotek PLGEL-Mixed B columns 30 cm long, with an internal diameter of 7.5 mm. The columns were protected by a guard column and an inline filter, and samples manually injected using a Rheodyne 200 um injection loop. Samples were prepared up to 1 mg ml^{-1} concentration and passed through a nylon syringe filter to remove any remaining undissolved particles. The samples were then injected into the machine individually for analysis. JordiGel sulphonated DVB columns were used for the chromatography, and sample's chromatogram was detected by using a HP 1047A refractive index (RI) and UV detectors. **Viscometry.** Viscosity average molecular weights of prepared polymers were also calculated using an Ostwald glass capillary viscometer thermostated at 30 °C.

Fluorescence Analysis. **Steady State Measurements.** Fluorescence steady state measurements were carried out on a Perkin-Elmer LS50 Luminescence Spectrometer or Spectrofluorometer FluoroMax®-4. Both emission measurements (λ_{ex} 320 nm, λ_{em} 360 - 510 nm) and excitation measurements (λ_{ex} 260-380 nm, λ_{em} 420 nm). Emission and excitation slits were set between 2.5 and 4nm depending on the analysed sample. Ten accumulation scans were made for each reading to ensure smooth spectra, giving an accuracy of each intensity ±5% CPS. **Time Correlated Single Photon Counting.** Fluorescence excited state lifetime and time resolved measurements were carried out via an IBH 5000 system and Edinburgh Instruments 199 Fluorescence Spectrometers, respectively using a nanoLED excitation source (λ_{ex} 370 nm) and a monochromator set to detect fluorescence emission (λ_{em} 450 nm). The detector analysed a time range of 100 ns and 30,000 counts were obtained for each sample for lifetime measurements and 20,000 counts were obtained for time resolved measurements. A silica prompt was run after each sample to consider scattered light from the source during fluorescence analysis. Fluorescence measurements were all made using 10^{-1} wt% polymer solutions with the water purified using Millipore simfilter equipment with the water being filtered at a resistance of 18.2M Ωcm^{-1}. The pH of the polymer

solutions was verified using NaOH and HCl with the pH being recorded on a pH meter.

Potentiometric Titrations. Potentiometric titrations were carried out on a Metrohm 718 STAT-Titrino instrument using a protocol outlined previously.[31] The titrations of polymers were carried out at 25 °C using NaCl (either 0.001, 0.01 or 1.0 M) as the background electrolyte. The polymer solution was prepared by dissolving a known amount of polymer in degassed ultrahigh quality (UHQ) water. The 0.1 M NaOH and 0.1 M HCl solutions were prepared from NaOH and HCl using UHQ water, and the exact concentration was determined prior to the titration against a primary standard $Na_2B_4O_7.10H_2O$. The samples were dissolved in 25 mL of NaCl electrolyte and the solution was purged with N_2 (> 99.99%) for 1 hour to remove CO_2 before initiating titration, yielding a constant pH value. Following the degassing procedure, a positive pressure of N_2 was maintained by allowing a gentle flow of N_2 into the headspace during the titration. The sample solutions were acidified to pH ≈ 2 using 0.1 M HCl and then titrated to pH ≈ 11 using 0.1 M NaOH. A blank without desired sample was also titrated. To assess reversibility and protonation behaviour, a reverse acidimetric titration was applied following the base titration. Each experiment was done 3 times. The titrator was set to add successive acid or base every 20 seconds. The electrode was standardized on a proton concentration scale, $[H^+]$, and the slope deviation from the theoretical Nernst value was always within 1%.

Inductively Coupled Plasma Mass Spectrometry analysis (ICP-MS)

The inductively coupled plasma mass spectrometer (ICP-MS, Perkin Elmer Elar 400 DRC II) was used to determine the mineral content of eluent following dilution and acidification with (1% v/v HNO_3).

Analysis

Loading of Fluorescence Label. The quantity of fluorescent label ($(mol\%)_{fluorophore}$) in the polymers was determined using the UV-Vis absorption of the polymer solution compared to stock solutions of the pure fluorophore. The mol% of the fluorescent label was calculated by the following equation:

$$(\mathrm{mol}\%)_{\mathrm{fluorophore}} = \frac{C_{\mathrm{fluorophore}}}{C_{\mathrm{fluorophore}}+C_{\mathrm{Monomer}}}\, x\, 100 \quad (1)$$

Where, $C_{fluorophore}$ and $C_{Monomer}$ are the molar concentration of the fluorescent label and the nonfluoro-monomer, respectively.

Fluorescent label content. A more accurate concentration (C) can be determined mathematically from the Beer-Lambert's law for the calibration curve as flows:

$$A = \mathcal{E}bC \quad (2)$$

Where, A is the absorbance value of fluorophore, Ɛ is the molar absorptivity; b is the bath length of the cell, equal to 1 cm and C the concentration of fluorescent label in solution.

Viscometry Average Molecular Weight. Measured viscosity values from the Ostwalf Viscometer were expressed in terms of reduced (η_{red}) and inherent (η_{inh}) as flows:

$$t_r = \frac{t_p}{t_s} \quad (3)$$

$$\rho_r = \frac{\rho_p}{\rho_s} \quad (4)$$

$$\rho_r\, x\, t_r = \eta_r \quad (5)$$

$$\eta_{sp} = \eta_r - 1 \quad (6)$$

$$\eta_{red} = \frac{\eta_{sp}}{C_p} \quad (7)$$

$$\eta_{inh} = \frac{\ln\eta_r}{C_p} \quad (8)$$

Where, t_r, t_p, and t_s represent the relative efflux time, the efflux time of aqueous polymer solution and the measured efflux time of solvent, respectively. And ρ_r, ρ_p and ρ_s represent the relative density, the density of aqueous polymer solution and the density of solvent, respectively. Whereas, η_r is the relative viscosity of aqueous polymer solution, η_{sp} is the specific viscosity, and C_p is the concentration (in mass per volume) of aqueous polymer solution. Plots of η_{sp} / C_p and ln η_r / C_p as a function of polymer concentration were constructed. The curves extrapolate to the intrinsic viscosity, [η], at zero concentration. The average viscosity molecular weight, $<M_v>$, was calculated according to the Mark-Houwink equation;

$$[\eta] = k\, x < M_v >^a \quad (9)$$

Where, K and a are constants for a given solvent and temperature.

Adsorption of polymers on alumina. Polymer solutions of the desired concentrations were prepared in aqueous solution and the solution pH adjusted as required. 10 ml of a polymer solution was then placed in 20 ml centrifuge tube and the necessary amount of alumina powder was added slowly while being stirred. The suspensions were then stirred or shaken overnight. After equilibration, samples were centrifuged at 5000 rpm for 40 minutes, and then the upper-level solution was taken and centrifuged at 5000 rpm for another 40 minutes. Aliquots of the supernatant were then carefully removed.

Adsorption of polymers on silica. Polymer and silica solutions were pH adjusted after mixing. The mixture was shaken overnight to ensure that adsorption had reached equilibrium. The solution was then centrifuged at 50000 rpm (Beckman Coulter Optima LE-80K Ultracentrifuge) for 2 hours to sediment the solid phase from the aqueous phase. The supernatant was then carefully withdrawn from the top of the centrifuge tube. Fluorescence steady state analysis was run of polymer mineral solution before and after separation and the

percentage of adsorbed polymer calculated from the fluorescence intensity.

Mineral Determination The ICP-MS was calibrated with samples of known concentration of alumina and silica. The equilibrated mineral polymer solution was transferred into ultrafiltration cylinder (pore size 1 kDa), free mineral was passed through the filter and collected in a flask. The eluent was diluted and acidified (1% v/v HNO3) and the ICP-MS analysis was carried out. The adsorbed mineral amount = the initial concentration – the free mineral. The ICP-MS was left to equilibrate for 1 hour between each measurement before being purged by a blank solution.

Results and Discussions

In order to characterise the behaviour and interactions of alginate with inorganic particles a fluorescent tag was covalently attached to it, resulting in a high yield of AmNS-alginate product. A 98% yield was achieved, and all chemical characterisation data are provided in the supporting information.

Characterisation of Alginates

Besides its poor solubility one of the problems characterising alginic acid (and similar) biopolymers are their conformational response to their environment.[29] The stimuli responsive properties of these materials are driven by the solvation shell of the polymer, which is in turn driven by its hydrophilicity. Computational modelling of both the M and G monomer (Figure 1A) show equivalent Log P potential (see supporting evidence) and as such little evidence that monomer composition should change stimuli responsive solution properties above the pKa. This is driven primarily by the fraction of carboxylic acid (COOH) groups on the mannuronic and guluronic acid backbone. The fractional dissociation (α) of these groups, with respect to varying ionic strengths of solution, was studied via a potentiometic titration as shown in Figure 1C. This titration showed that the polysaccharide demonstrates only weak polyelectrolyte activity and does not reach full ionisation or deionisation unless outside of the pH range 2 – 11. The degree of deprotonation is dependent on the ionic strength of the solution however, as the higher NaCL concentration (1 M) showed ≈60% deprotonation by pH 4 whereas in more dilute solutions (0.1 and 0.01 M) this was only ≈ 40%. The counter ion salts of the supernatant appear to mitigate the internal electronegative repulsion of the polymer chain that counters ionisation above the functional group pka. Data for the pKa values of both the original and dye labelled alginate show the addition of the fluorescent tag has not altered the inflection point for any transition, and as such indicates that that the physicochemical behaviour for the labelled alginate is similar to that unlabelled biopolymer.

Physicochemical Behaviour of Alginate* in Aqueous Solution

Both the fluorescence intensity and excited state lifetime of dilute AmNS aqueous solutions are quenched in acidic conditions (< pH 7), with no further response as the pH is increased above pH 11, and in all studies the emission wavelength and dynamic behaviour remained unaffected (see ESI Section 2). Furthermore, regardless of pH, addition of AmNS solution (10-5 M) to a 1 wt% solution of silica or alumina led to no change in the solution absorbance prior to mixing or after the solid components were removed by centrifugation, nor a change in the correlation time of the dye – indicating that there is no interaction between the AmNS and the mineral particles

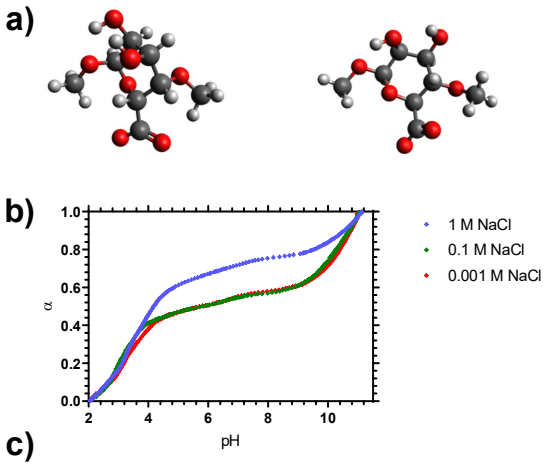

c)

NaCl (M)	$pKa_{(COOH)}$	$pKa_{(C\text{-}OH)}$	$pKa_{(C\text{-}NH2)}$	pHzpc
0.1	3.38	7.00	10.00	2.35
0.1	3.40	7.06	9.60	2.38

Figure 1. Top: Structure of G (left) and M (right) monomers from computational modelling used to determine LogP. Middle: Fraction of acid groups ionized versus pH as a function of NaCl concentration for alginic acid. Bottom: pKa Constants and pH_{zpc} of labelled and unlabelled alginates as determined by titration curves.

(see ESI section 3). The AmNS labelled Alginate* was also prepared as a dilute solution (10^{-1} wt %) and It showed an increased response to pH, indicating that the covalently attached dye was able to act as a reporter on the conformational behaviour of the macromolecule in solution (Figure 2). Alginate* shows a reduction in both fluorescence intensity (Figure 2A) and an increase in the excited state lifetime (Figure 2B) above pH 9 that is not observed in the free dye, and furthermore when compared to the fluorescence intensity in neutral solutions (pH 7) the drop of intensity at pH 3 is more pronounced. The fluorescence lifetime of AmNS was recorded in a range of solvents and it typically increased in hydrophilic solvents compared to non-polar ones (for example τ_f = 11.4 ns in water compared to 7.0 ns in butanol). Therefore the sharper decay of the Alginate* at pH 2 can be attributed to it's non-polar environment due to the collapsed polymer chain. This indicates the presence of the alginate macromolecule is having a pronounced impact in multiple different ways upon the fluorescence processes of the AmNS dye. The enhancement of fluorescence intensity from pH 5 to 10 could be attributed to the existence of the hydrophilic fluorophore in an aqueous environment as the chain expands, whilst the

quenching above pH 9 arises from dynamic quenching by OH^- ions which is likely exacerbated by the close proximity of functional groups on the polymer backbone. This quenching has been observed on the free dye in solution but only initiating above pH 11 as opposed to a slow increase from pH 9 - 12.[32]

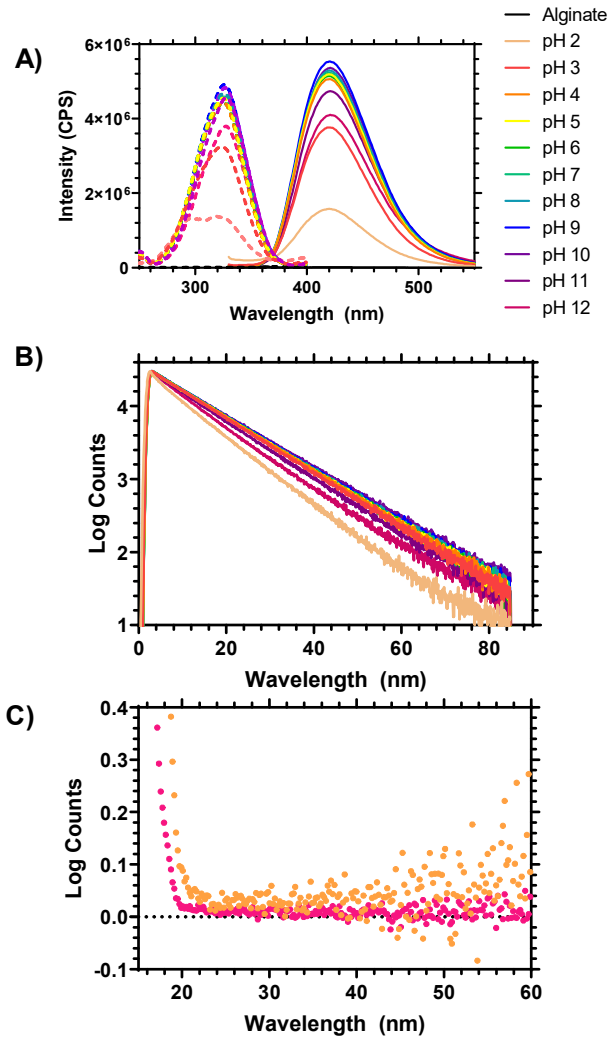

Figure 2. A) Fluorescence emission spectra for 10^{-1}w% Alginate* in water as a function of pH at λ_{ex}= 320 nm. B) Fluorescence intensity decays for 10^{-1}w% Alginate* in water as a function of pH at λ_{ex}= 370 nm and λ_{em}= 450 nm. C) Decay of anisotropy, r(t), of 10^{-1} wt% Alginate* in aqueous solution at pH 2 (blue line) and pH 12 (red line). (λ_{ex} = 370nm and λ_{em} = 450nm).

The chain mobility of alginate in aqueous solutions was examined using TRAMS (Figure 2C). Unlike the intensity and decay data this showed a linear progression in the anisotropic profiles changing from pH2 to 12 that reflected the chain mobility of the Alginate*. When the intensity and anisotropic decays (Figure 2B-C) were fitted to extract τ_f and τ_c a full profile of the Alginate* pH responsiveness becomes apparent, particularly compared to the free AmNS component (Figure 3). This data indicates that the mobility of the macromolecule is restricted when the alginate chain is coiled in acidic media, resulting in quenching on the fluorescent dye and restricted segmental mobility of the covalently attached dye.

Figure 3 displays the relative fluorescence intensity (compared to pH 7), the fluorescence lifetime and rotational correlation time of alginate* and AmNS as a function of pH. This shows that with increasing pH the chain mobility of alginate increases (i.e. reducing τ_c value) whilst the fluorescence lifetime and intensity of the due increase respectively up to pH 9. The pH dependence observed in Figure 3 implies that the mobility of the collapsed alginate chain is slower than that of the partly expanded chain.

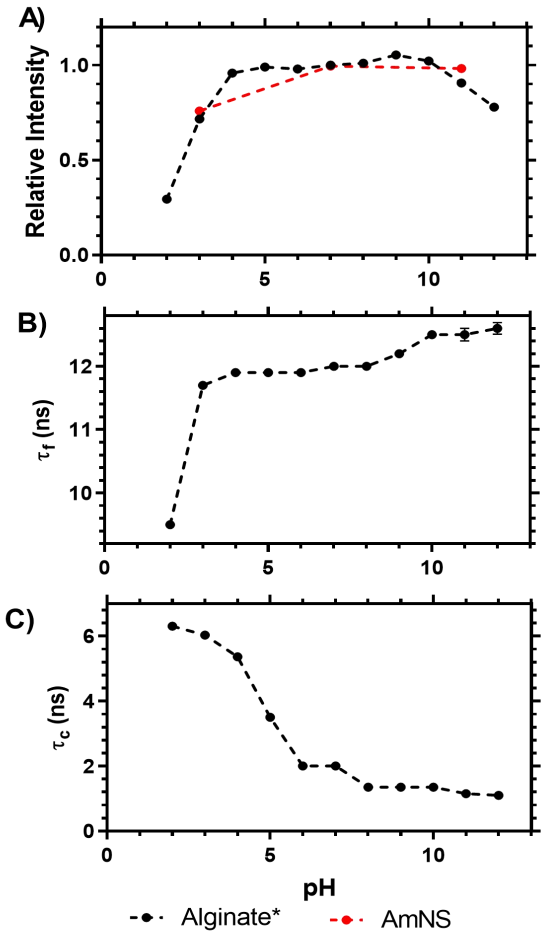

Figure 3 A) Relative Fluorescence intensity (to intensity at pH 7) B) Fluorescence lifetime C) Correlation times(τ_c) for molecular segmental motion of 10^{-1} wt% Alginate* in aqueous solution at different pH values. (λ_{ex}=370nm and λ_{em}=450nm).

Conformational Behaviour of Alginate*

The interaction of the alginate with monovalent and divalent salt solutions was studied to demonstrate the impact of ionic strength on the polymer conformation. As the confirmational change of the alignate is driven by deprotonation changes in the electrostatic repulsion due to the ionic strength of the

solution can alter this transition, screening the negative charge and causing a transition from to a partially coiled state. The alginate* still exhibited pH responsive fluorescence with only minor differences in emission compared to the original polymer (see ESI section 5).

Figure 4 shows the graphs of τ_c against the addition of different concentrations of NaCl and $CaCl_2$ to alginate* solutions at pH 3 and 9. With increasing concentration (0.0001 M to 5 M), the correlation time of the NaCl solution increased (7 to 30 ns), whereas the $CaCl_2$ solution showed a more dramatic change (7 to 70 ns) within a narrower molar concentration range (up to 1.5 M).

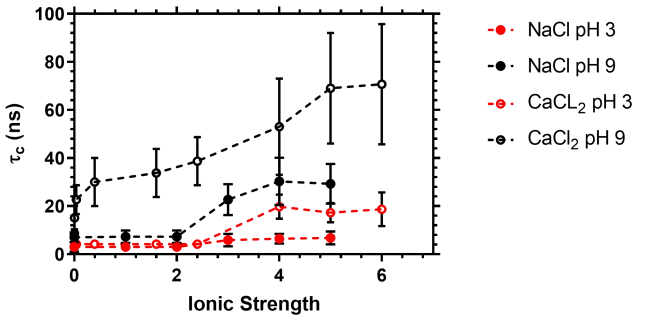

Figure 4 Correlation times (τ_c) for molecular segmental motion of 10^{-1} wt% Alginate* in aqueous solution in different A) NaCl B) $CaCL_2$ concentration(M) at pH9 (blue curve) and pH 3 (red curve). (λ_{ex}=370nm, λ_{em}=450nm).

There is evidence that the anionic COO^- groups and CO^- moieties in polyelectrolytes have electrostatic repulsions that are shielded by Na^+ at pH 9.[33,34] This may result in the screening of electrostatic repulsion throughout the alginate chain. As a result, the expanded coils move faster than the collapsed biopolymer chains. This has previously been observed in the context of changes in the viscosity of a polysaccharide solution. It has been reported that the intrinsic viscosity of polysaccharide solutions decreases with increasing salt concentration in basic medium, indicating that at high salt concentrations, the electrolyte polysaccharide chains assume coiled conformations.[35] Ca^{2+} ions have a known interaction with the COO^- and CO^- groups of alginic acid.[33,34,36] The interaction with Ca^{2+} ions is favoured because the COOH and C-OH groups are deprotonated at pH 9 compared to neutral groups at pH 3. However, this interaction charges the carboxylate and alkoxy groups and causes the natural polyelectrolyte chain to collapse, inhibiting the motion of the AmNS-alginate chain. AFM has previously been used to investigate the chelation of calcium cations by alginate COO^- groups.[37] The addition of Ca^{2+} ions transformed the alginate solution into a thin gel, indicating that the anionic polysaccharide chains adopt coiled conformations in the presence of $CaCl_2$ salt. FTIR analysis of other studies has revealed that both the COOH and C-OH functional groups in alginate are involved in metal binding.[36]

Adsorption of Alginate* on Silica Surface as a Function of pH

Fluorescence steady state and anisotropy measurements were carried out on the AmNS-alginate at different silica concentration as a function of pH, with confidence that the free AmNS remains dispersed into the bulk solution and does not interact with silica after separation. Fluorescence steady-state spectroscopy was used to quantify the adsorbed amount of biopolymer on silica particles, while TRAMS was applied to investigate the dynamic behaviour of adsorbed alginate.

Figure 5A shows the amount of adsorbed biopolymer (as percentage) as a function of pH and silica concentration. As an overall trend, the amount of adsorbed biopolymer increases by decreasing the pH from 11 to 2. The analysis of surface charge of alginate and silica with the change of pH is essential to clarify the obtained dependencies. The zero point of charge of alginate is 2.83,[38] whereas it is ~3 of silica.[39–41] It means that apart from pH 2 the surfaces of SiO_2 and alginate are negatively charged in the completely studied pH range changing from 2 to 11. Under such conditions, the electrostatic repulsion between alginate chains and the silica particles takes place. pH increase causes the decrease of biopolymer adsorption due to electrostatic repulsion between the COO^- groups in alginate and the negatively charged silanol groups on the silica particle is strengthened. The adsorption of alginate on the silica surface could be attributed to that non-electrostatic forces appear between alginate and the silica surface. Otherwise, the interaction of similarly charged materials should not occur.[41] X-ray photoelectron spectroscopy (XPS) and atomic force microscopy (AFM) have been used in the literature to characterize the adsorption of alginic acid to TiO_2 surface (pH_{zpc}~5) as a function of solution pH.[26] It was found that alginic acid adsorbs in greater quantity at acidic pH than at basic pH.

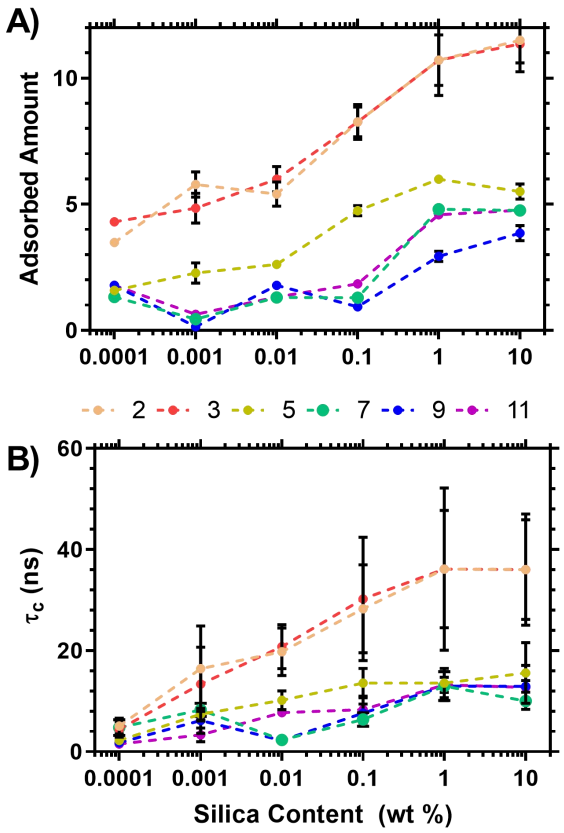

Figure 5. A) Adsorption of alginate* on the silica as a function of silica concentration at various pH values. Concentration of biopolymer in the solution is 10^{-1} wt %. B) Correlation times of alginate* as a function of silica concentration at various pH values.

In contrast, increasing the amount of SiO_2 leads to an increase in the amount of adsorbed polysaccharide. At low silica concentration, from 10^{-4} to 10^{-2} wt %, there is a slight increase in the adsorbed amount of alginic acid at pH 2 and 3, whereas no important adsorption was noted at pH levels 5, 7, 9 and 11. A gradual increase was recorded when the silica concentration was increased to 10 wt% at pH 2 and 3. Under these conditions, 11 % was the maximum percentage of the biopolymer attachment to silica particles. Although this amount is considered small it is well within the sensitivity of fluorescence analysis.

Generally, the correlation time increased with decreasing pH from 11 to 2, but increasing the amount of silica led to an increase in the τ_c values. Definitely at a low concentration of silica, from 10^{-4} to 10^{-2} wt%, there was a gradual increase in the correlation time values at pH 2 and 3, but no important change was recorded at pH values 5,7,9 and 11. Then again, an obvious rise was identified when the silica content increased to 1 wt% at pH 2 and 3. At 10 wt% of silica the correlation time remained approximately constant, this can be explained with saturation between the natural polyelectrolyte chain and the silica. However, a small increase was recorded at pH values, 5,7,9 and 11 for silica concentration range from 10^{-1} to 10 wt%.

Adsorption of Alginate* on Alumina surface as a function of pH

Figure 6A presents the percentage amount of adsorbed alginate as a function of pH and alumina concentration. In general, the amount of adsorbed biopolymer increases when the pH drops from 11 to 2. The pH dependence of the adsorption could be attributed to the biopolymer and mineral pHzpc values, which are 2.83 and ~ 9, respectively. It means that apart from pH 9 and 11 the surface of alumina is positively charged, while the alginate is negatively charged in the pH range from 3 to 11. As a result, the electrostatic attraction between alginate chains and the alumina particles takes place at the pH values 7, 5 and 3. pH decrease causes the increase of biopolymer adsorption due to electrostatic attraction between the COO^- groups in alginate and the positively charged alumina groups when both the biopolymer and alumina have the same kind of charge (i.e. at pH 9 and 11).At pH 2 and 3, besides the non-electrostatic forces, potential hydrogen bonding could be responsible for the adsorption and resultant reduction in biopolymer rotational diffusion (Figure 6B).

The effect of pH on the adsorption of PAA (a typical model for alginate) to alumina has been reported elsewhere.[42] It was found that a higher adsorption at the lower pH. This means that the surface of alumina is positively charged, while polyelectrolyte is negatively charged. Moreover, electrostatic interactions between the polyelectrolyte and the alumina surface play a key role in the adsorption of polymer. On contrary, the biopolymer adsorption increases by increasing the quantity of added mineral (from 10^{-4} to 10 wt %). Specifically, a gradual increase in the adsorbed alginate at pH values of 5, 7, 9 and 11. Whereas, a marked increase was

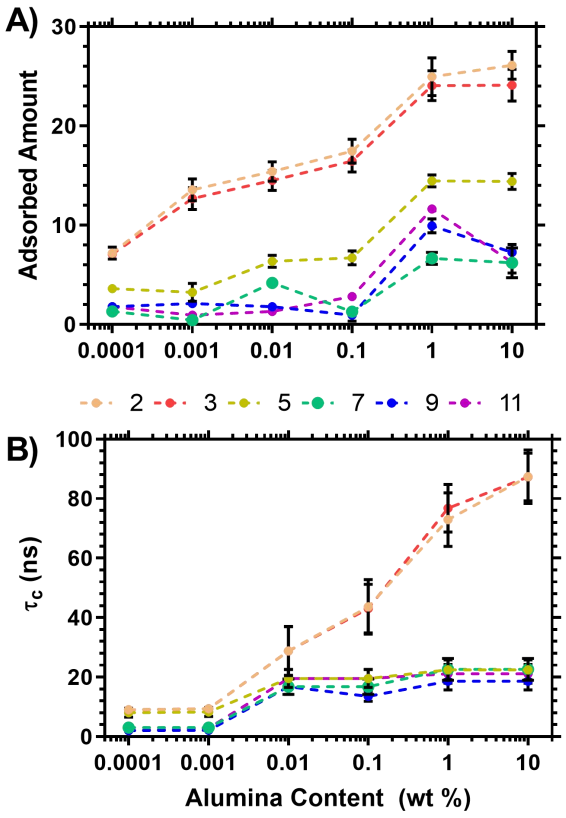

Figure 6. A) Adsorption of alginate* on the alumina as a function of alumina concentration at various pH values. Concentration of biopolymer in the solution is 10^{-1} wt%. B) Correlation times of alginate* as a function of alumina concentration at various pH values.

observed at pH 2 and 3, as the percentage of adsorbed alginate reaches the maximum value (~26%). Under such conditions only ~11 % of biopolymer was adsorbed on silica. This could be attributed to that within acidic media the alginate is neutralised and the biopolymer chain is more collapsed in an adsorbed state. Thus, unionised carboxylic acid (COOH) and hydroxyl (C-OH) groups adsorb via hydrogen bonding between the biopolymer carbonyl group and hydroxyls on alumina surface. Hence, at lower pH values the adsorption mechanism is predominantly hydrogen bonding in nature, whereas alginate does not adsorb significantly onto silica due to electrostatic repulsion.

Figure 6B displays the correlation times (τ_c) of AmNS-labelled-alginate (10^{-1} wt %) as a function of alumina concentration at different pH values. It can be observed that from 10^{-4} to 10^{-2} wt% of alumina concentration there is a slight increase in the τ_c values over the whole pH range, this suggests a weak adsorption where the AmNS label exists in a semi homogeneous environment, since the vast majority of alginate chains are not adsorbed. In such cases, a single exponential fit is suitable to calculate the correlation time values in nanoseconds. A double exponential fit was selected to analyse the anisotropy decays at a concentration of alumina content equal to 0.1 wt % at pH 2 and 3, where the biopolymer partially adsorbs onto alumina, which means that the AmNS label is dispersed in two phases, solid and bulk solution. When the alumina concentration is increased to 10 wt %, an increase is recorded at pH 2 and pH 3, which means a strong adsorption occurs. In this case, a single exponential function was also believed to be suited to fit such anisotropy decays.

The variation in the relative charge density of silica and alumina particles in the absence and presence of adsorbed alginate is illustrated in Figure 7. As it can be concluded clearly, the adsorption of the anionic polysaccharide decreases the positive charge considerably and lowers the pH_{zpc} of the alumina from ~ 9 to 8.4, whereas no effect on the relative charge behaviour of silica suspension is recorded, since the pH_{zpc} of the silica remains non shifted at ~3. These results propose that electrostatic interactions are predominantly responsible for the adsorption of alginic acid on Al_2O_3 molecules, whereas weak forces, such as Van der Waals assumed to control the interference between alginate and SiO_2 suspension. Since in acidic condition, the fluorescence experiment showed that the percentage of adsorbed natural polyelectrolyte reaches the value (~26%) on alumina, while only ~11% on silica. This is because at low pH levels (i.e. pH = 3) the net charge on alumina is positive and alginate is negatively charged, whereas the silica particles are neutral.

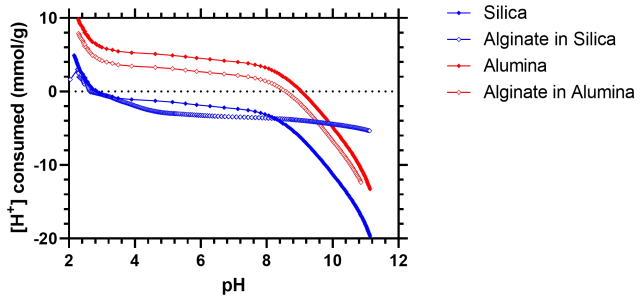

Figure 7. Relative surface charge versus pH for silica, alumina, alginate in alumina and alginate in silica.

Inductively Coupled Plasma Mass Spectrometry Measurements (ICP-MS) of Silica and Alumina Adsorption on Alginate

The results obtained from the fluorescence spectroscopy showed that a reasonable amount of fluorescently labelled biopolymer adsorbs on the surface of alumina in acidic media, but fewer adsorbs on silica suspension under the same conditions. Moreover, the increase in the quantity of solid added leads to an increase in the alginate adsorption. However, in this section, the ICP-MS is applied to quantify the adsorbed minerals on unlabelled alginic acid according to the procedure, outlined in the experimental part.

Figure 8A shows the pH dependence for the adsorption of Al_2O_3 and SiO_2 on unlabelled alginate. As it can be observed, for the two examined minerals, the adsorption of alumina and

silica on alginate increase when the pH of the solution is reduced from 11 to 2. However, the rate of increment in these amounts for silica is less than in those for alumina. The effect of pH on the adsorbed amounts can be explained based on the type of the interaction of charged mineral with the polyelectrolyte chain. At pH lower than pH_{zpc} of alumina (~9), the alumina is positively charged and the net charge on the alginate chain is negative. Because of that, the increase of alumina adsorption (from pH 7 to pH 3) could be attributed to that electrostatic attraction between the oppositely charged materials. A decline in the adsorption of alumina at pH higher 9 occurs because of the electrostatic repulsion between the negatively charged alumina and anionic polysaccharide. This adsorption behaviour coincides with the recent polyelectrolyte adsorption theory established by Van der Schee and Lyklema,[43] which can be summarized as follows: adsorption of a negatively or partly negatively charged macromolecule on a positively charged mineral is influenced by electrostatic forces.

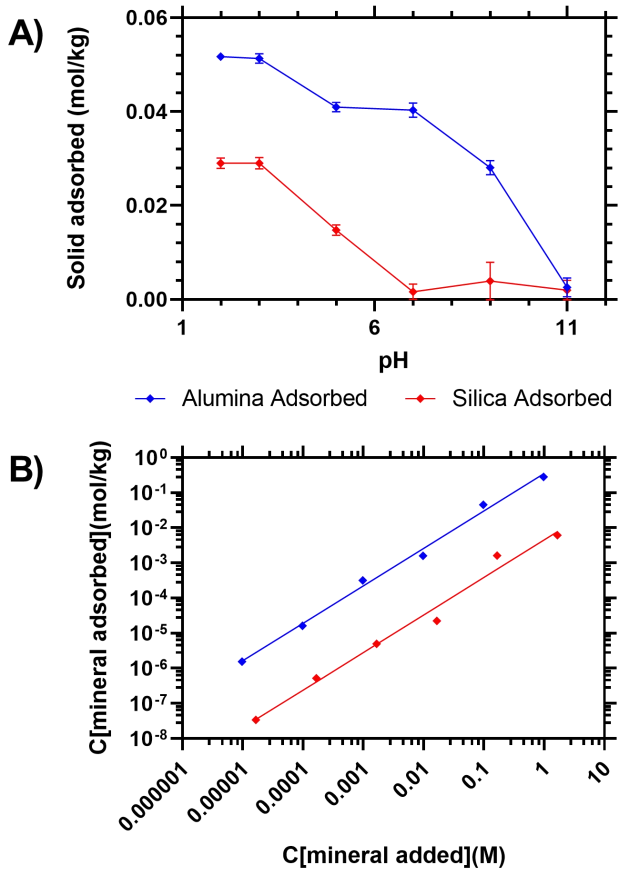

Figure 8. Top: Effect of pH on the adsorption of alumina and silica on alginate (solid added 0.1 M. Bottom: Henry adsorption isotherms of alumina and silica on alginate, at pH 7.

Interestingly, the alginate chain can adsorb on the alumina, as well as the silica particles over the entire studied pH range, even at pH values where which both the biopolymer and the solid have electrostatic repulsion, indicating strong nonionic interactions between the mineral and the polyelectrolyte.[44]

In addition to particle charge, mineral concentration influences the adsorption process of minerals on natural polyelectrolyte. The alumina and silica isotherms plots representing the adsorbed amounts of minerals on the alginate were obtained at pH 7 by varying the added concentration of minerals (~10^{-5} to 1 M). These adsorption measurements were carried out at the same concentration of biopolymer (10^{-1} wt %). The adsorbed amount of alumina on alginate increased markedly with increasing concentration of alumina in the liquid phase at pH 7. On the other hand, the shape of the isotherm suggests a weaker affinity of alginate for silica (the adsorbed amounts are lower than alumina over the entire concentration range). This means that at pH 7 the electrostatic attraction enhanced the adsorption of alumina. For example, at added concentration of ~1 *M*, the adsorbed amount of alumina on alginate is ~0.3 mol/kg, which is about 50 times greater than the adsorbed amount of silica on alginate. The obtained isotherms were fitted to the Henry adsorption model as shown in Figure 8B. These linear dependencies enable calculation of the affinity constant (K_h) of minerals adsorption from the slope of the Henry's equation. The obtained K_h and goodness of fit (R^2) values are given in Table 1. Considering the values of R^2 the Henry model is good to describe such isotherms. The K_h of the Henry model represents a measure of adsorption affinity. A large value of K_h reflects stronger adsorption. It can be noted that, over the complete pH range the affinity of minerals to adsorb on the polysaccharide chain increases by decreasing the pH of solution. This could also attribute to the attraction of oppositely charged materials. However, under the identical condition Al_2O_3 particles have a greater affinity for the alginate than SiO_2 suspensions. This is due to the effects of the zero point of charge for minerals. The most efficient adsorption occurred at lower pH values, under these conditions, where the alumina particles hold a positive charge, so that they are strongly attracted to negatively charged alginate and generate larger Henry's constant values. Silica suspensions have a weak affinity for biopolymer because of the electrostatic repulsion of negative silica molecules with anionic polyelectrolytes.

Table 1. Henry (affinity) constants of alumina and silica adsorbed on alginate and the goodness of fit values, at different pH values.

pH	K_h (L/kg) (Alumina)	R^2 (Alumina)	K_h (L/kg) (Silica)	R^2 (Silica)
2	0.5751	0.9999	0.1367	0.9868
3	0.5898	0.9998	0.1004	0.9598
5	0.2934	0.9977	0.0818	0.9485
7	0.2896	0.9954	0.0039	0.9659
9	0.0027	0.9999	0.0037	0.9706
11	0.0041	0.9993	0.0033	0.9909

Discussion:

It can be noted that the pH (and ionic strength) dependence of the conformation of alginic acid is clearly similar to the behaviour of synthetic poly (acrylic acid) discussed in our previous work.[28] The pH dependence of the conformation of the alginate chain is also in agreement with recent research, which reports the aggregation of alginic acid occurring at pH less than 4.1.[22] We compared the Henry (affinity) constants of the alginates with the previously published results for the synthetic polymer poly(acrylic acid) and found that they had equivalent affinities for alumina particles between pH 3 and 7, and comparable (but slightly lower) affinities to silica from pH 2 – 7 (see supporting information for full comparisons).

This work was carried out at low ionic strength conditions, and whilst our data shows that the alginate is conformationally susceptible to higher ionic strengths there is no evidence to suggest whether the fundamental binding interactions would be affected.

Log P has been shown to be a useful guide for gauging the hydrophilicity (and thus solution properties) of polymer systems.[45] As the log p has been shown to vary with chain length the modelling of short chain segments indicates the increased hydrophilicity of the alginate gives it less baseline affinity for inorganic particles than the synthetic acrylate polymer. Alternatively, the COO^- groups of the alginate biopolymer could be more sterically hindered than the synthetic polymer further reducing the effective interaction. However despite this comparison the alginate material still performed well at adsorbing the pollutant particles and is both a cheap, cost effective and biodegradable alternative to the synthetic material.

Conclusions

This work has shown that alginate is an effective biopolymer for isolation and subsequent removal of the main inorganic constituents of fly ash particles from water at low to intermediate pH. The data evidences that fluorescence time resolved anisotropy is a powerful technique for the study of the conformational behaviour of dilute alginate solutions, and for determining their attachment to solid surfaces. In comparison, fluorescence steady state and lifetime measurements were less informative due to quenching of the AmNS label under acid conditions. From pH 5 to 10 (> *pKa* of AmNS) the fluorescence intensity and lifetime of the label are quenched. Consequently, the observed dependence of the fluorescence intensity and lifetime with pH was attributed to a change in conformation of the alginate chain. Fluorescence steady-state experiments showed that a greater amount of the fluorescently labelled alginate adsorbs onto the surface of alumina (~26%) in acidic media, in contrast to that onto silica (~11%) at the same pH. The correlation time, τ_c, of the labelled alginate increases as the amount of solid increases and the pH decreases: this suggests that more sites on the biopolymer chain is occupied by solid, which leads to restricted fluorophore and consequently macromolecular mobility. The results obtained from potentiometric analysis suggested that electrostatic interactions were predominantly responsible for the adsorption of alginate on Al_2O_3 particles, whereas weak forces, such as Van der Waals are assumed to control the interference between the polysaccharide chain and SiO_2 suspension. The adsorption affinity of alginate for alumina is due to electrostatic attraction between the positively charged alumina and the negatively charged alginate. In contrast, an electrostatic repulsion is responsible for the adsorption of alginate.

Conflicts of interest

There are no conflicts to declare.

Acknowledgements

A. SA. A. thanks Taif University Research Supporting Project number (TURSP-2020/44) Taif University, Taif, Saudi Arabia. F. E. acknowledges the support of University of Benghazi, Benghazi, Libya. Dr Thomas Swift thanks the Royal Society of Chemistry for funding to carry out analytical comparisons (E21-8346952505).

References

1 A. B. and V. M. Malhotra, High-Volume Fly Ash System: Concrete Solution for Sustainable Development, *ACI Mater. J.*, , DOI:10.14359/804.

2 R. K. Singh, N. C. Gupta and B. K. Guha, Fly Ash Disposal in Ash Ponds: A Threat to Ground Water Contamination, *J. Inst. Eng. Ser. A*, 2016, **97**, 255–260.

3 M. M. Khachan, S. K. Bhatia, B. W. Maurer and A. C. Gustafson, Dewatering and Utilization of Fly Ash Slurries Using Geotextile Tubes, *Indian Geotech. J.*, 2012, **42**, 194–

205.
4 A. Dwivedi and M. K. Jain, Fly ash–waste management and overview: A Review, *Recent Res. Sci. Technol.*
5 V. K. Jha, M. Matsuda and M. Miyake, Resource recovery from coal fly ash waste: an overview study, *J. Ceram. Soc. Japan*, 2008, **116**, 167–175.
6 C.-F. Lin and H.-C. Hsi, Resource recovery of waste fly ash: synthesis of zeolite-like materials, *Environ. Sci. Technol.*, 1995, **29**, 1109–1117.
7 V. K. Yadav and M. H. Fulekar, Advances in methods for recovery of ferrous, alumina, and silica nanoparticles from fly ash waste, *Ceramics*, 2020, **3**, 384–420.
8 X. Sun, J. Li, X. Zhao, B. Zhu and G. Zhang, A review on the management of municipal solid waste fly ash in American, *Procedia Environ. Sci.*, 2016, **31**, 535–540.
9 R. Xu, T. Lyu, L. Wang, Y. Yuan, M. Zhang, M. Cooper, R. J. G. Mortimer, Q. Yang and G. Pan, Utilization of coal fly ash waste for effective recapture of phosphorus from waters, *Chemosphere*, 2022, **287**, 132431.
10 H. Yangthong, S. Wisunthorn, S. Pichaiyut and C. Nakason, Novel epoxidized natural rubber composites with geopolymers from fly ash waste, *Waste Manag.*, 2019, **87**, 148–160.
11 P. Li, X. Dou, M. Müller, C. Feng, M. W. Chang, M. Frettlöh and H. Schönherr, Autoinducer Sensing Microarrays by Reporter Bacteria Encapsulated in Hybrid Supramolecular-Polysaccharide Hydrogels, *Macromol. Biosci.*, , DOI:10.1002/mabi.201700176.
12 A. Zanoletti, I. Vassura, E. Venturini, M. Monai, T. Montini, S. Federici, A. Zacco, L. Treccani and E. Bontempi, A new porous hybrid material derived from silica fume and alginate for sustainable pollutants reduction, *Front. Chem.*, 2018, **6**, 60.
13 N. Uzma and M. Datta, Adsorption Studies of Zinc (II) Ions On Biopolymer Composite Beads of Alginate-Fly Ash, 2014, **3**, 682–691.
14 J. E. Gregor, E. Fenton, G. Brokenshire, P. Van Den Brink and B. O'sullivan, Interactions of calcium and aluminium ions with alginate, *Water Res.*, 1996, **30**, 1319–1324.
15 L. Li, Y. Fang, R. Vreeker, I. Appelqvist and E. Mendes, Reexamining the egg-box model in calcium− alginate gels with X-ray diffraction, *Biomacromolecules*, 2007, **8**, 464–468.
16 J. Yang, S. Chen and Y. Fang, Viscosity study of interactions between sodium alginate and CTAB in dilute solutions at different pH values, *Carbohydr. Polym.*, 2009, **75**, 333–337.
17 H. Zhang, H. Zheng, Q. Zhang, J. Wang and M. Konno, The interaction of sodium alginate with univalent cations, *Biopolym. Orig. Res. Biomol.*, 1998, **46**, 395–402.
18 K. I. Draget, G. Skjåk-Bræk, B. E. and Christensen, O. Gåserød and O. Smidsrød, Swelling and partial solubilization of alginic acid gel beads in acidic buffer, *Carbohydr. Polym.*, 1996, **29**, 209–215.
19 K. I. Draget, B. T. Stokke, Y. Yuguchi, H. Urakawa and K. Kajiwara, Small-angle X-ray scattering and rheological characterization of alginate gels. 3. Alginic acid gels, *Biomacromolecules*, 2003, **4**, 1661–1668.
20 T. Coradin, N. Nassif and J. Livage, Silica–alginate composites for microencapsulation, *Appl. Microbiol. Biotechnol.*, 2003, **61**, 429–434.
21 W. Jiao, W. Chen, Y. Mei, Y. Yun, B. Wang, Q. Zhong, H. Chen and W. Chen, Effects of molecular weight and guluronic acid/mannuronic acid ratio on the rheological behavior and stabilizing property of sodium alginate, *Molecules*, 2019, **24**, 4374.
22 Y. Cao, X. Shen, Y. Chen, J. Guo, Q. Chen and X. Jiang, pH-induced self-assembly and capsules of sodium alginate, *Biomacromolecules*, 2005, **6**, 2189–2196.
23 I. A. Oberyukhtina, K. G. Bogolitsyn and N. P. Popova, Physicochemical properties of solutions of sodium alginate extracted from brown algae Laminaria digitata, *Russ. J. Appl. Chem.*, 2001, **74**, 1645–1649.
24 O. Smidsrød, Solution properties of alginate, *Carbohydr. Res.*, 1970, **13**, 359–372.
25 E. R. West, M. Xu, T. K. Woodruff and L. D. Shea, Physical properties of alginate hydrogels and their effects on in vitro follicle development, *Biomaterials*, 2007, **28**, 4439–4448.
26 R. A. Brizzolara, Adsorption of alginic acid to titanium investigated using x-ray photoelectron spectroscopy and atomic force microscopy, *Surf. Interface Anal. An Int. J. devoted to Dev. Appl. Tech. Anal. surfaces, interfaces thin Film.*, 2002, **33**, 351–360.
27 A. J. de Kerchove and M. Elimelech, Structural growth and viscoelastic properties of adsorbed alginate layers in monovalent and divalent salts, *Macromolecules*, 2006, **39**, 6558–6564.
28 D. J. Sparks, M. E. Romero-González, E. El-Taboni, C. L. Freeman, S. A. Hall, G. Kakonyi, L. Swanson, S. A. Banwart and J. H. Harding, Adsorption of poly acrylic acid onto the surface of calcite: An experimental and simulation study, *Phys. Chem. Chem. Phys.*, 2015, **17**, 27357–27365.
29 F. Eltaboni, E. Caseley, M. Katsikogianni, L. Swanson, T. Swift, M. Romero-Gonzalez, F. El-Taboni, E. Caseley, M. Katsikogianni, L. Swanson, T. Swift and M. E. Romero-González, Fluorescence Spectroscopy Analysis of the Bacteria–Mineral Interface: Adsorption of Lipopolysaccharides to Silica and Alumina, *Langmuir*, , DOI:10.1021/acs.langmuir.9b02158.
30 J. C. G. Blonk, J. Van Eendenburg, M. M. G. Koning, P. C. M. Weisenborn and C. Winkel, A new CSLM-based method for determination of the phase behaviour of aqueous mixtures of biopolymers, *Carbohydr. Polym.*, 1995, **28**, 287–295.
31 J. J. Ojeda, M. E. Romero-González, R. T. Bachmann, R. G. J. Edyvean and S. A. Banwart, Characterization of the cell surface and cell wall chemistry of drinking water bacteria by combining XPS, FTIR spectroscopy, modeling, and potentiometric titrations, *Langmuir*, 2008, **24**, 4032–4040.
32 J. FICK, R. LAWACZECK and F. W. SCHNEIDER, Fluorescence of Intramolecular and Intermolecular Interactions of Aminonaphthyl-sulfonate with Nucleotides, *Eur. J. Biochem.*, 1982, **126**, 367–372.

33 K. L. Chen, S. E. Mylon and M. Elimelech, Aggregation kinetics of alginate-coated hematite nanoparticles in monovalent and divalent electrolytes, *Environ. Sci. Technol.*, 2006, **40**, 1516–1523.

34 K.-P. Kim, Z. Ahmed, K.-G. Song, S. F. Magram, M. H. H. Daoud, K.-H. Ahn and K.-J. Paeng, Adsorption of aluminum ion from water on alginate-modified polyurethane, *J. Chem. Eng. Japan*, 2011, 1101050107.

35 K. Tsutsumi and T. Norisuye, Excluded-volume effects in sodium hyaluronate solutions revisited, *Polym. J.*, 1998, **30**, 345–349.

36 E. Torres, Y. N. Mata, M. L. Blázquez, J. A. Munoz, F. González and A. Ballester, Gold and silver uptake and nanoprecipitation on calcium alginate beads, *Langmuir*, 2005, **21**, 7951–7958.

37 A. W. Decho, Imaging an alginate polymer gel matrix using atomic force microscopy, *Carbohydr. Res.*, 1999, **315**, 330–333.

38 C. Jeon, J. Y. Park and Y. J. Yoo, Characteristics of metal removal using carboxylated alginic acid, *Water Res.*, 2002, **36**, 1814–1824.

39 A. A. Zaman, R. Tsuchiya and B. M. Moudgil, Adsorption of a low-molecular-weight polyacrylic acid on silica, alumina, and kaolin, *J. Colloid Interface Sci.*, 2002, **256**, 73–78.

40 W. M. Carty and U. Senapati, Porcelain—raw materials, processing, phase evolution, and mechanical behavior, *J. Am. Ceram. Soc.*, 1998, **81**, 3–20.

41 M. Wiśniewska, Temperature effect on adsorption properties of silica-polyacrylic acid interface, *J. Therm. Anal. Calorim.*, 2010, **101**, 753–760.

42 Z. Pan, A. Campbell and P. Somasundaran, Polyacrylic acid adsorption and conformation in concentrated alumina suspensions, *Colloids Surfaces A Physicochem. Eng. Asp.*, 2001, **191**, 71–78.

43 H. A. Van Der Schee and J. Lyklema, A lattice theory of polyelectrolyte adsorption, *J. Phys. Chem.*, 1984, **88**, 6661–6667.

44 A. V. Dobrynin and M. Rubinstein, Effect of Short-Range Interactions on Polyelectrolyte Adsorption at Charged Surfaces †, *J. Phys. Chem. B*, 2003, **107**, 8260–8269.

45 S. Varlas, J. C. Foster, L. A. Arkinstall, J. R. Jones, R. Keogh, R. T. Mathers and R. K. O'Reilly, Predicting monomers for use in aqueous ring-opening metathesis polymerization-induced self-assembly, *ACS Macro Lett.*, 2019, **8**, 466–472.